

# The Nuclear Contact Formalism – the Deuteron Channel

Ronen Weiss<sup>1</sup> and Nir Barnea<sup>1,\*</sup>

<sup>1</sup>*The Racah Institute of Physics, The Hebrew University, Jerusalem, Israel*

(Dated: October 29, 2021)

The contact formalism, devised to elucidate the important role of short-range correlations, was recently generalized for systems with coupled channels, such as the deuteron channel, where  $s$  and  $d$  waves are coupled into a  $J = 1$  state. The coupling of the two channels implies two independent asymptotic solutions and results a  $2 \times 2$  contact matrix. For a strong coupling, with appropriate boundary conditions, such as in nuclear physics, the two solutions degenerate into a single asymptotic wave function. Here, we explore the asymptotic behavior of the correlated neutron-proton pairs in the deuteron channel using both schematic models and realistic nuclear forces.

PACS numbers: 67.85.-d, 05.30.Fk, 25.20.-x

*Introduction* – Short range correlations (SRCs) are known to play an important role in nuclear physics. High-momentum tail ( $k > k_F \approx 1.26 \text{ fm}^{-1}$ ) originated by SRCs was identified in different nuclei both in theory and in experiment, see *e.g.* [1–5], and also [6, 7] for reviews. Nuclear systems are complicated systems, composed of protons and neutrons, each with a spin degree of freedom. In the study of SRCs in nuclear systems there are many indications and a wide agreement in the literature on the fact that, due to the tensor force, nuclear SRCs are dominated by proton-neutron (pn) pairs, that can be described to a good approximation using the single  $T = 0$  deuteron bound state [2, 3, 8–12]. The cross section of electron-scattering experiments, sensitive to SRCs, is approximately proportional to the deuteron cross-section [4, 5, 13]. Also, the  $pn$  momentum distribution, calculated numerically in [1] for different nuclei, is approximately a multiplication of the deuteron momentum distribution [14, 15]. Recently, the high momentum-tail of the one-body momentum distribution of  $A \leq 40$  nuclei was reproduced using the contact formalism [16], where the main contribution comes from the deuteron channel, using the single bound state wave function.

The contact formalism is a theoretical tool for analyzing SRCs in quantum systems. The contact was initially introduced to describe systems of two-component fermions, obeying the zero-range condition [17]. Later on, it was generalized to study nuclear systems [14, 16, 18–22]. Nuclear systems do not obey the zero range condition, and as a result the contribution of all partial waves should be considered, not only the  $s$ -wave contribution, and model dependent functions must be used instead of the known zero-range two-body functions. As a result, the nuclear contact matrices were defined and new relations between different nuclear quantities, which are sensitive to nuclear SRCs, were revealed and verified [14–16, 18, 20, 22]. Contact matrices and contributions from different partial waves were also considered recently to describe SRCs in other systems [23–25].

In [26] the contact formalism was extended to describe systems that, like the deuteron, are dominated by cou-

pled channels. It was found that for  $n$ -coupled channels, the contact is replaced by an  $n \times n$  matrix, connecting all possible asymptotic partial waves. Therefore, instead of a universal tail to the momentum distribution, such as the  $1/k^4$  tail found by Tan for zero-range interaction [17], one expect a superposition of universal terms, each having a different asymptotic behavior.

This result seems to stand in contrast with the observation that a universal deuteron-like tail dominates nuclear SRCs. That is, the freedom suggested by the contact matrix of two different asymptotic functions is somehow suppressed, and we are left with a single function. To explain this phenomena, it was observed in [26] that by imposing a box-like boundary condition on the low energy spectrum, the contact matrix collapses into a single constant in the limit of strong coupling. This means that for a strong coupling between the different channels, the boundary condition at long distance determines the short range behavior. For finite nuclei, such a boundary condition can be understood as the effective attraction induced by the surrounding nucleons on the correlated pair.

To gain more insight into the asymptotic behavior of correlated neutron-proton pairs, we will explore here with some detail the asymptotic behaviour of a deuteron-like system composed of  $s$  and  $d$ -waves coupled into a  $J = 1$  state. To this end, we will first review the formalism and some of the main results of [26], and then present further analysis of the two-body density and two-body momentum distribution using both “toy model” and realistic nucleon-nucleon (NN) interactions.

*Coupled channels contact formalism* – Consider a nuclear system composed of  $A$  nucleons. In such a system, when two neutrons  $n, n'$  approach each other, we expect the total wave function  $\Psi(\mathbf{r}_1, \dots, \mathbf{r}_A)$  to be dominated by the asymptotic form

$$\Psi \xrightarrow{r_{nn'} \rightarrow 0} \varphi(\mathbf{r}_{nn'}) A(\mathbf{R}_{nn'}, \{\mathbf{r}_k\}_{k \neq n, n'}). \quad (1)$$

where,  $\mathbf{r}_k$  are the single-particle coordinates,  $\mathbf{r}_{nn'} = \mathbf{r}_n - \mathbf{r}_{n'}$ ,  $\mathbf{R}_{nn'} = (\mathbf{r}_n + \mathbf{r}_{n'})/2$ ,  $\varphi(\mathbf{r})$  is the universal

spin-scalar  $\ell = 0$  zero-energy solution of the Schrödinger equation of two neutrons, and  $A(\mathbf{R}_{nn'}, \{\mathbf{r}_k\}_{k \neq n, n'})$  is a regular function describing the dynamics of all other nucleons.

When considering also higher partial waves, if the different channels are not coupled, the asymptotic form becomes [14, 23]

$$\Psi \xrightarrow{r_{nn'} \rightarrow 0} \sum_{\alpha} \varphi_{\alpha}(\mathbf{r}_{nn'}) A^{\alpha}(\mathbf{R}_{nn'}, \{\mathbf{r}_k\}_{k \neq n, n'}). \quad (2)$$

The sum over  $\alpha$  indicates the different channels, which in the case of two nucleons are given by  $\alpha = (\ell, s)j m$ . When considering coupled channels, the quantum numbers indicated by  $\alpha$  are not necessarily sufficient to describe the universal part of the asymptotic wave-function.

To illuminate the difference between the coupled and uncoupled cases we shall focus on the deuteron channel. Generalization of the following arguments to any other channels is strait forward. For a neutron-proton pair, residing in a deuteron-like state, the wave function is composed of an  $s$  and  $d$  channels, given by  $|s\rangle = |(\ell = 0, s = 1)j = 1 m\rangle$  and  $|d\rangle = |(\ell = 2, s = 1)j = 1 m\rangle$ , and the general solution to the Schrödinger equation is a superposition of two independent solutions,

$$\varphi^a(\mathbf{r}) = \varphi_s^a(r)|s\rangle + \varphi_d^a(r)|d\rangle. \quad (3)$$

The indices  $a = 1, 2$  stands for the two independent solutions. Each of these solutions is a mixture of both channels,  $|s\rangle$  and  $|d\rangle$ . Now it is evident that when a neutron  $n$  and a proton  $p$  approach each other, the asymptotic wave function, dominated by the deuteron channel, will take the form

$$\Psi \xrightarrow{r_{np} \rightarrow 0} \sum_{a=1,2} \varphi^a(\mathbf{r}_{np}) A^a(\mathbf{R}_{np}, \{\mathbf{r}_k\}_{k \neq n, p}). \quad (4)$$

Notice that it is different than the asymptotic form given in Eq. (2), since Eq. (4) includes two different functions  $\varphi_s^1(r)$  and  $\varphi_s^2(r)$ , and each of them is generally coupled to a different  $A^a$  function. Since the nuclear wave function  $\Psi$  has a well-defined total angular momentum  $J$ , a summation over  $m$  is also required here (see Ref. [14]). We omit it here for simplicity, since it does not affect our conclusions.

The above asymptotic form leads to the definition of a  $2 \times 2$  contact matrix for the case of two coupled channels:

$$C^{ab} = 16\pi^2 NZ \langle A^a | A^b \rangle, \quad (5)$$

where  $a, b = 1, 2$ . Notice that  $A^1$  and  $A^2$  are generally not orthogonal. Previous studies, that have defined a matrix of contacts [14, 24, 25], implicitly assumed that asymptotically the potential does not couple different channels.

As presented in [26], this asymptotic form and contact matrix can be used to derive different contact relations. We review the deuteron-channel contribution to the momentum and density distributions. The single-particle

momentum distribution,  $n(k) = \int d\hat{k} n(\mathbf{k})$ , describing the probability to find a particle with momentum  $k$ , is given asymptotically by

$$n(k) \xrightarrow{k \rightarrow \infty} \sum_{a,b=1,2} (\tilde{\varphi}_s^{a*}(k) \tilde{\varphi}_s^b(k) + \tilde{\varphi}_d^{a*}(k) \tilde{\varphi}_d^b(k)) \frac{C^{ab}}{16\pi^2}, \quad (6)$$

where  $n(\mathbf{k})$  is normalized to the number of nucleons in the system  $A$ , and  $\tilde{\varphi}_{\alpha}^a(k)$  is the Fourier transform of  $\varphi_{\alpha}^a(r)$ . The two-particle momentum distribution  $F(k) = \int d\hat{k} F(\mathbf{k})$ , which describes the probability to find an  $np$  particle pair with relative momentum  $k$ , is given by

$$F(k) \xrightarrow{k \rightarrow \infty} \sum_{a,b=1,2} (\tilde{\varphi}_s^{a*}(k) \tilde{\varphi}_s^b(k) + \tilde{\varphi}_d^{a*}(k) \tilde{\varphi}_d^b(k)) \frac{C^{ab}}{16\pi^2}. \quad (7)$$

Finally, the asymptotic probability to find a pair of  $pn$  particles with relative distance  $r$ ,  $\rho(r) = \int d\hat{r} \rho(\mathbf{r})$ , is given by

$$\rho(r) \xrightarrow{r \rightarrow 0} \sum_{a,b=1,2} (\varphi_s^{a*}(r) \varphi_s^b(r) + \varphi_d^{a*}(r) \varphi_d^b(r)) \frac{C^{ab}}{16\pi^2}. \quad (8)$$

$\rho(r)$  and  $F(k)$  are normalized to the number of pairs.

From these results it is evident that if the two solution  $\varphi^a$ ,  $a = 1, 2$ , have different asymptotic forms, then, depending on the explicit form of the contact matrix (5), each nucleus might have a different asymptotic momentum or density distributions. For example, if we will compare two different eigenstates,  $\Psi_1$  and  $\Psi_2$ , and look on the ratio of the two corresponding momentum distributions,  $n_1(k)/n_2(k)$ , this ratio will generally not obtain a constant value for high momentum. This is because the values of the different four contacts  $C^{ab}$  can be different for each state, and the  $k$ -dependence will not generally disappear, same for  $F(k)$  and  $\rho(r)$ . As mentioned before, this is the result that seems to contradict the universal deuteron-like behavior of nuclear SRCs. Since nuclear momentum and density distributions are reproduced using the single bound-state deuteron wave function, such a ratio of two distributions will have an asymptotic constant behavior, in contrast to the discussion above.

In a mean field picture, the nucleons in the atomic nucleus are subject to an attractive potential whose magnitude is of the order of  $\epsilon_F \approx 30$  MeV. Consequently, the universal wave function  $\varphi$ , Eq. (3), is also subject to such an attractive potential, and all bound nucleon pairs will have an exponentially-decaying long-range tail. This effect of the mean field potential was approximated in [26] through hard wall boundary condition. There, it was found that if the coupling between the  $s$  and  $d$  channels is strong enough, as is the case for nuclear-physics, all the low-laying two-body states with energy below about 30 MeV have the same asymptotic form.

Consequently, considering only the deuteron-channel

contribution, in finite nuclei it is expected that

$$n(k) \xrightarrow[k \rightarrow \infty]{} (\tilde{\varphi}_s^{*D}(k)\tilde{\varphi}_s^D(k) + \tilde{\varphi}_d^{*D}(k)\tilde{\varphi}_d^D(k)) \frac{C}{16\pi^2}, \quad (9)$$

$$F(k) \xrightarrow[k \rightarrow \infty]{} (\tilde{\varphi}_s^{*D}(k)\tilde{\varphi}_s^D(k) + \tilde{\varphi}_d^{*D}(k)\tilde{\varphi}_d^D(k)) \frac{C}{16\pi^2}, \quad (10)$$

and

$$\rho(r) \xrightarrow[r \rightarrow 0]{} (\varphi_s^{*D}(r)\varphi_s^D(r) + \varphi_d^{*D}(r)\varphi_d^D(r)) \frac{C}{16\pi^2}, \quad (11)$$

where  $\varphi_s^D(r), \varphi_d^D(r)$  are the  $s, d$  components of the deuteron wave function, and  $\tilde{\varphi}_s^D(k), \tilde{\varphi}_d^D(k)$  are their Fourier transform. This result solves the contradiction between the known nature of nuclear SRCs and the predictions of the coupled-channels contact theory.

*The asymptotic wave-function* – To solve the Schrödinger equation for the coupled  $s, d$ -channels we can integrate the radial equation from  $r = 0$  outwards starting with one of the two distinct boundary conditions

$$\begin{aligned} \frac{d(r\varphi_s^1)}{dr} = 1 & & \frac{d^3(r\varphi_d^1)}{dr^3} = 0 \\ \frac{d(r\varphi_s^2)}{dr} = 0 & & \frac{d^3(r\varphi_d^2)}{dr^3} = 1. \end{aligned} \quad (12)$$

For a scattering, positive energy, case there are no further conditions on the wave-function, and therefore  $\varphi^1, \varphi^2$  or any linear combination

$$\varphi(\mathbf{r}) = c_1 \begin{pmatrix} \varphi_s^1(r) \\ \varphi_d^1(r) \end{pmatrix} + c_2 \begin{pmatrix} \varphi_s^2(r) \\ \varphi_d^2(r) \end{pmatrix}, \quad (13)$$

with  $c_1$  and  $c_2$  being free coefficients, are legitimate physical solutions. Adding a bound-state boundary condition of a vanishing wave-function at  $r \rightarrow \infty$  leads to energy quantization, and for each allowed energy there is only one solution characterized by the value of the ratio  $\eta \equiv c_2/c_1$ .

In order to see the implications of such a boundary condition, we will first use the simple “toy model” composed of a simple gaussian potential with  $s, d$  coupling introduced in [26],

$$\begin{aligned} V_{s,s} = V_{d,d} &= -V_0 \exp(-\Lambda^2 r^2) \\ V_{s,d} = V_{d,s} &= -SV_0 \exp(-\Lambda^2 r^2) \end{aligned} \quad (14)$$

and solve the Schrödinger equation for this potential in a spherical hard wall box of radius  $R$ . For a given strength  $S$ ,  $V_0$  is tuned to produce a constant scattering length, and the ratio of  $\eta_i$  for the  $i^{\text{th}}$  energy level is extracted from the corresponding wave function. The results for the ratio  $|\eta_1(S) - \eta_2(S)|/|\eta_1(S) + \eta_2(S)|$  comparing the  $\eta$  values of the first two energy levels are presented in Fig. 1. The calculations were done for scattering length  $a_s = 10$  fm and different values of

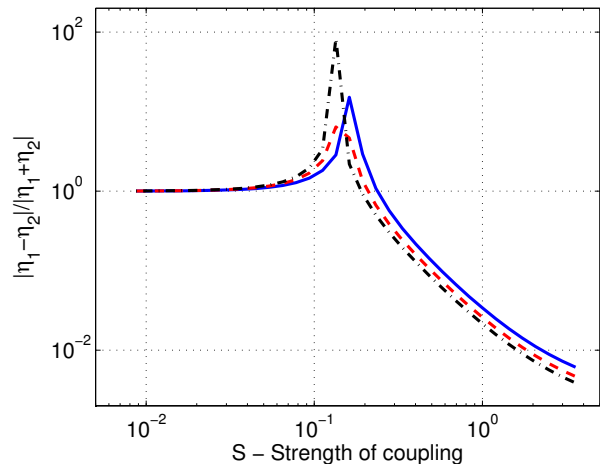


FIG. 1. Comparison between the values of  $\eta(E) \equiv c_2(E)/c_1(E)$  for the first two allowed energies in a box with radius  $R$  as a function of  $S$ , using the simple “toy model” potential. We used  $\Lambda^2 = 3 \text{ fm}^{-2}$  and the scattering length was kept constant  $a_s = 10$  fm. The blue, red and black lines are for  $R = 15, 25, 35$  fm.

$R$ . In the non-coupling limit  $S \rightarrow 0$ , the lowest energy state is a pure  $s$ -wave,  $\eta \rightarrow 0$ , and the  $2^{\text{nd}}$  excited state is a pure  $d$ -wave,  $\eta \rightarrow \infty$ . Consequently the ratio  $|\eta_1(S) - \eta_2(S)|/|\eta_1(S) + \eta_2(S)| \rightarrow 1$ , as can be seen in the figure. On the other hand, as was already observed in [26], the ratio  $|\eta_1(S) - \eta_2(S)|/|\eta_1(S) + \eta_2(S)| \rightarrow 0$  as the coupling  $S$  becomes stronger and stronger, which means that the short-range behavior of the two wavefunctions become identical in the strong-coupling limit ( $\eta_1 \approx \eta_2$ ). It should be emphasized that this phenomenon is due to the boundary condition at  $R$ , and does not depend on the exact value of  $R$ . For scattering states there is always a complete freedom to choose the parameters  $c_1$  and  $c_2$  at will.

We now turn to study the effect of the coupling strength on the density. In Fig. 2 we present the densities of the two lowest energy states obeying box boundary condition, with two different coupling values  $S = 0.2$  and  $S = 2$ . The calculation was carried out for a fixed scattering length  $a_s = 10$  fm. In this figure it can be seen that for the strong coupling ( $S = 2$ ),  $\rho(r)$  is similar for these two energy states up to almost  $r = 0.8$  fm. On the other hand, for  $S = 0.2$ , the solutions corresponding to the two states behave differently starting from a smaller distance, around  $r \approx 0.3$  fm. The similar behavior for smaller distances is because in such small distances only the  $s$ -wave component of the solutions is significant, while the  $d$ -wave component goes to zero in the origin. We therefore deduce that also in an  $A$ -body system with intermediate values of coupling strength, when two particles get close to each other, they are not restricted to behave like the bound “deuteron”, but rather as any of

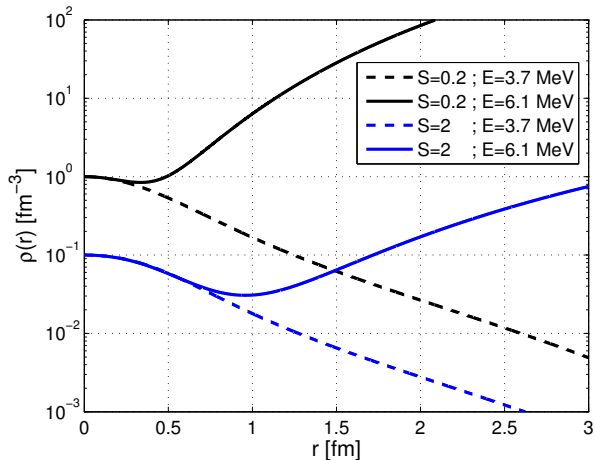


FIG. 2. The densities of the two lowest energy states in the “toy model” with a box boundary condition at  $R = 15$  fm, and  $S = 0.2$  or  $S = 2$ . The scattering length was fixed to  $a_s = 10$  fm, and  $\Lambda^2 = 3 \text{ fm}^{-2}$ .

the two solutions. As the coupling becomes stronger, a convergence towards unique short range behavior is again observed.

Now, let us turn and study the implications of the boundary condition on the neutron-proton momentum distribution using the realistic NN potential model AV18 [27] and the chiral EFT force N3LO(600), see [28] and ref. therein. To this end, we have solved the Schrödinger equation in an external harmonic oscillator (HO) potential, that simulates the effective mean field potential the nucleons fill inside the nucleus. Similar to the box boundary condition, this external potential also leads to the quantization of the continuum solutions. In figures 3 for AV18 and 4 for N3LO(600), we present the normalized momentum distributions ratios

$$\left( \frac{n_l(k)}{n_D(k)} \right) \left( \frac{\rho_D(0)}{\rho_l(0)} \right)$$

of the first 10 levels (subscript  $l$ ) compared to the deuteron solution (subscript  $D$ ), where  $\rho$  is the coordinate-space density. The levels spread the energy range  $-2.2 \text{ MeV} \leq E_l \leq 20 \text{ MeV}$ , due to the value of  $\hbar\omega_{HO} = 0.1 \text{ MeV}$ . One can see that also here, due to the external potential, all the low energy continuum solutions are similar to the bound deuteron solution for large momenta. We note that the two different nucleon-nucleon potentials used in these calculations lead to the same conclusion.

Inspecting the figures, one can observe the grouping of the levels into two color groups having slightly different behavior at the momentum range  $1.5 \text{ fm}^{-1} \leq k \leq 2.5 \text{ fm}^{-1}$ . This grouping can be attributed to the different  $\eta$  values. For  $k \geq 2.5 \text{ fm}^{-1}$  all the solutions collapse into a single solution proportional to the deuteron. One

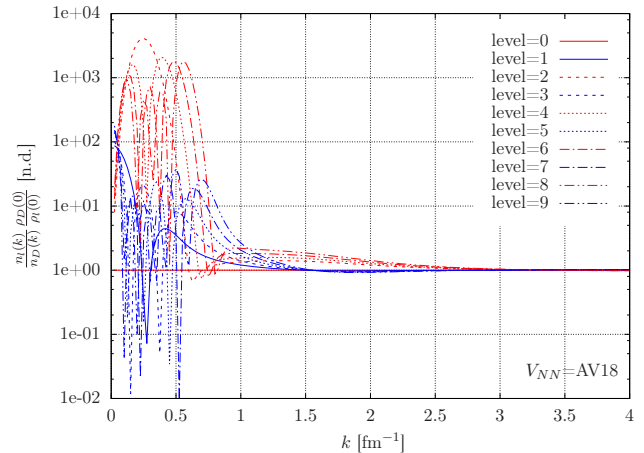


FIG. 3. Momentum distribution ratios for the first few two-body levels in an external HO potential. Here we have used the AV18 NN potential.

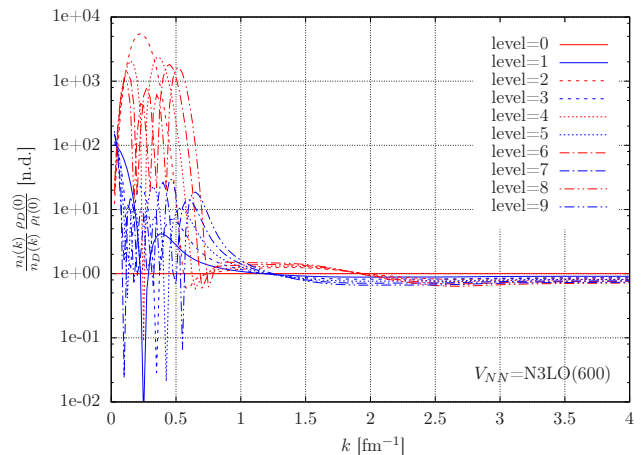


FIG. 4. Momentum distribution ratios for the first few two-body levels in an external HO potential. Here we have used the chiral EFT N3LO(600) NN potential.

might argue that what we see is the  $s$ -wave dominance, however, it should be noted that at  $k \approx 4 \text{ fm}^{-1}$  the  $s$ -wave and  $d$ -wave contributions to  $n(k)$  are roughly equal.

*Summary* – Summing up, we have seen here and in [26], that without imposing a boundary condition at  $r \rightarrow \infty$ , the contact formalism for two coupled channels requires a  $2 \times 2$  contact matrix and two asymptotic functions. This seems to contradict the known features of nuclear SRCs that are dominated by the deuteron channel with the single bound-state deuteron wavefunction. Adding such a boundary condition resolve this tension, because, in the strong-coupling limit, it results in a collapse of the contact matrix to a single contact and a single asymptotic function. This boundary condition can be interpreted as the effective mean-field potential applied on

the correlated pair due to the remaining particles in the nucleus. In the case of a weak coupling, two asymptotic functions are still generally needed.

Using a “toy model” and a hard-wall boundary condition, it was shown that for a strong coupling term in the potential, the densities of the two lowest energy states coincide over a significant range. In addition, using two different realistic nuclear forces, and in the presence of an external HO potential (instead of the hard wall), the asymptotic momentum distribution of the first few positive energy solutions coincide with the bound-state deuteron high-momentum tail. This indicates that the collapse to a single asymptotic wave function in the strong-coupling limit is a general phenomenon, independent of the exact NN potential or boundary condition.

This work was supported by the Pazy Foundation.

---

\* [nir@phys.huji.ac.il](mailto:nir@phys.huji.ac.il)

- [1] R. B. Wiringa, R. Schiavilla, S. C. Pieper, J. Carlson, Phys. Rev. C **89**, 024305 (2014).
- [2] O. Hen et al. (CLAS Collaboration), Science **346**, 614 (2014).
- [3] M. Alvioli, C. Ciofi degli Atti and H. Morita, Phys. Rev. Lett. **100**, 162503 (2008).
- [4] N. Fomin et al., Phys. Rev. Lett. **108**, 092502 (2012).
- [5] J. Arrington, D. Higinbotham, G. Rosner, M. Sargsian, Prog. Part. Nucl. Phys. **67**, 898 (2012).
- [6] C. Ciofi degli Atti, Phys. Rep. **590**, 1 (2015).
- [7] O. Hen, G.A. Miller, E. Piasetzky, and L. B. Weinstein, Rev. Mod. Phys. **89**, 045002 (2017)
- [8] E. Piasetzky, M. Sargsian, L. Frankfurt, M. Strikman, J.W. Watson, Phys. Rev. Lett. **97**, 162504 (2006).
- [9] R. Subedi *et al.*, Science **320**, 1476 (2008).
- [10] R. Schiavilla, R. B. Wiringa, Steven C. Pieper, and J. Carlson, Phys. Rev. Lett. **98**, 132501 (2007).
- [11] I. Korover, *et al.*, Phys.Rev.Lett. **113**, 022501 (2014).
- [12] H. Baghdasaryan, *et al.*, Phys. Rev. Lett. **105**, 222501 (2010).
- [13] L.L. Frankfurt, M.I. Strikman, D.B. Day, M. Sargsyan Phys.Rev. C **48**, 2451 (1993)
- [14] R. Weiss, B. Bazak, and N. Barnea, Phys. Rev. C **92**, 054311 (2015).
- [15] M. Alvioli, C. Ciofi degli Atti, and H. Morita, Phys. Rev. C **94**, 044309 (2016)
- [16] R. Weiss, R. Cruz-Torres, N. Barnea, E. Piasetzky, and O. Hen, arXiv:1612.00923 [nucl-th] (2017)
- [17] S. Tan, Ann. Phys. (N.Y.) **323**, 2952 (2008); **323**, 2971 (2008); **323**, 2987 (2008).
- [18] R. Weiss, B. Bazak, and N. Barnea, Phys. Rev. Lett. **114**, 012501 (2015).
- [19] O. Hen, L. B. Weinstein, E. Piasetzky, G. A. Miller, M. M. Sargsian, and Y. Sagi, Phys. Rev. C **92**, 045205 (2015).
- [20] R. Weiss, B. Bazak, and N. Barnea, Eur. Phys. J. A **52**, 92 (2016)
- [21] C. Bao-Jun, and Li. Bao-An, Phys. Rev. C **93**, 014619 (2016).
- [22] R. Weiss, E. Pazy, and N. Barnea, Few-Body Syst **58**, 9 (2017)
- [23] M. He, S. Zhang, H. M. Chan, and Q. Zhou, Phys. Rev. Lett. **116**, 045301 (2016)
- [24] S. Zhang, M. He, and Q. Zhou, arXiv:1606.05176 [cond-mat.quant-gas] (2016)
- [25] S. M. Yoshida and M. Ueda, Phys, Rev. A **94**, 033611 (2016)
- [26] R. Weiss and N. Barnea, Phys. Rev. C **96**, 041303(R) (2017).
- [27] R. B. Wiringa, V. G. J. Stoks, and R. Schiavilla, Phys. Rev. C **51**, 38 (1995).
- [28] E. Epelbaum, H. -W. Hammer and U. -G. Meißner, Rev. Mod. Phys. **81**, 1773 (2009).